Doublet stimulation increases Ca^{2+} binding to troponin C to ensure rapid force development in skeletal muscle

Anthony J. Bakker,[1]* Tanya R. Cully,[2]* Catherine D. Wingate,[1] Christopher J. Barclay,[3] and Bradley S. Launikonis[2]

[1]School of Anatomy, Physiology, and Human Biology, University of Western Australia, Perth, WA 6009, Australia
[2]School of Biomedical Sciences, University of Queensland, Brisbane, QLD 4072, Australia
[3]School of Allied Health Sciences, Griffith University, Gold Coast, QLD 4222, Australia

Fast-twitch skeletal muscle fibers are often exposed to motor neuron double discharges (≥200 Hz), which markedly increase both the rate of contraction and the magnitude of the resulting force responses. However, the mechanism responsible for these effects is poorly understood, likely because of technical limitations in previous studies. In this study, we measured cytosolic Ca^{2+} during doublet activation using the low-affinity indicator Mag-Fluo-4 at high temporal resolution and modeled the effects of doublet stimulation on sarcoplasmic reticulum (SR) Ca^{2+} release, binding of Ca^{2+} to cytosolic buffers, and force enhancement in fast-twitch fibers. Single isolated fibers respond to doublet pulses with two clear Ca^{2+} spikes, at doublet frequencies up to 1 KHz. A 200-Hz doublet at the start of a tetanic stimulation train (70 Hz) decreases the drop in free Ca^{2+} between the first three Ca^{2+} spikes of the transient, maintaining a higher overall free Ca^{2+} level during first 20–30 ms of the response. Doublet stimulation also increased the rate of force development in isolated fast-twitch muscles. We also modeled SR Ca^{2+} release rates during doublet stimulation and showed that Ca^{2+}-dependent inactivation of ryanodine receptor activity is rapid, occurring ≤1ms after initial release. Furthermore, we modeled Ca^{2+} binding to the main intracellular Ca^{2+} buffers of troponin C (TnC), parvalbumin, and the SR Ca^{2+} pump during Ca^{2+} release and found that the main effect of the second response in the doublet is to more rapidly increase the occupation of the second Ca^{2+}-binding site on TnC (TnC_2), resulting in earlier activation of force. We conclude that doublet stimulation maintains high cytosolic Ca^{2+} levels for longer in the early phase of the Ca^{2+} response, resulting in faster saturation of TnC_2 with Ca^{2+}, faster initiation of cross-bridge cycling, and more rapid force development.

INTRODUCTION

During cyclic muscular activity in vivo, mammalian motor units are characterized by patterns of excitation that commence with two or sometimes three high-frequency action potentials (up to 200 Hz) followed by a series of relatively low-frequency (20–80 Hz) stimuli. These so-called "doublet" excitation patterns have been observed in rodents (Hennig and Lømo, 1985; Gorassini et al., 2000) and humans (Desmedt and Godaux, 1977) and typically involve fast-twitch motor units (Zehr and Sale, 1994). Doublet discharges can increase tetanic force output by 44% and decrease contraction times by 50% compared with controls (Burke et al., 1976; see Binder-Macleod and Kesar [2005] for a review), a phenomenon that has been described by some as the "catch-like" property of skeletal muscle (Burke et al., 1970).

Doublet stimulation is reported to enhance force production by significantly elevating SR Ca^{2+} release (Duchateau and Hainaut, 1986). More recently, Cheng et al. (2013) used the Ca^{2+}-sensitive dye indo-1 to show that an initial 200-Hz doublet action potential results in a transient increase in peak tetanic free [Ca^{2+}] during the first 15 ms of the response that was ∼100% greater than that elicited at a stimulation rate of 70 Hz alone. Cheng et al. (2013) concluded that the increased peak free Ca^{2+} observed in response to a doublet stimulus reflected an increased release of Ca^{2+} in response to the second pulse. Similar reasoning was used to explain the effects of triplet stimulation on SR Ca^{2+} release (Abbate et al., 2002).

These studies suggest that doublet stimulation significantly increases initial Ca^{2+} release. However, to obtain an increase in SR Ca^{2+} release during doublet stimulation, the Ca^{2+} released in response to the second stimulation must be greater than the first, which is incompatible with previous studies showing a marked decrease in Ca^{2+} release shortly after an initial release caused by Ca^{2+}-dependent inactivation of the ryanodine receptors (CDI; Baylor and Hollingworth, 2003; Capote et al., 2005; Barclay, 2012). For these reasons, we suspected that limitations in previous tracking of cytosolic

*A.J. Bakker and T.R. Cully contributed equally to this paper.
Correspondence to Anthony J. Bakker: tony.bakker@uwa.edu.au; or Bradley S. Launikonis: b.launikonis@uq.edu.au
Abbreviations used: $[Ca^{2+}]_C$ (t), cytosolic Ca^{2+} transient; CDI, Ca^{2+}-dependent inactivation of the ryanodine receptors; EDL, extensor digitorum longus; EMG, electromyography; TnC, troponin C.

The Rockefeller University Press $30.00
J. Gen. Physiol. 2017 Vol. 149 No. 3 323–334
https://doi.org/10.1085/jgp.201611727

Ca^{2+} over time (cytosolic Ca^{2+} transient: $[Ca^{2+}]_C$ (t)) caused by the use of a high-affinity Ca^{2+} indicator and insufficient temporal resolution (500 Hz) have resulted in a distorted view of the tetanic Ca^{2+} response in previous studies (Abbate et al., 2002; Cheng et al., 2013) and led to erroneous conclusions.

Although doublet stimulation may not be increasing SR Ca^{2+} release, the pattern of Ca^{2+} signaling activated is likely to be altered in a way that enhances the activity of the force generation system. Therefore, the relationship between $[Ca^{2+}]_C$ (t) and the binding of Ca^{2+} to the contractile regulatory sites of the contractile apparatus needs to be taken into consideration when trying to interpret changes in $[Ca^{2+}]_C$ (t) in relation to SR Ca^{2+} release and to understand the physiological mechanisms responsible for the effects of doublet stimulation on force development. In fast-twitch muscle, any initial, rapid succession of action potentials releasing Ca^{2+} to the cytoplasm needs to result in binding of Ca^{2+} to two sites on troponin C (TnC; of different affinities) to induce contraction. The kinetics of Ca^{2+} binding to the TnC sites during high-frequency stimulation events such as doublets has not been explored, in part because the changes in $[Ca^{2+}]_C$ (t) during doublet stimulation have not been clearly defined with appropriate temporal resolution.

The aims of this study were first to accurately determine the time course of changes in free Ca^{2+} concentration in response to constant frequency and doublet stimulation and second to estimate the underlying differences in SR Ca^{2+} release and binding to TnC in response to the different stimulation protocols. To achieve the first of these aims, changes in free Ca^{2+} were measured using a fast, low-affinity Ca^{2+} indicator allied with high temporal resolution laser-scanning microscopy. The second aim was addressed by mathematical modeling of the release and distribution of Ca^{2+} in fibers in response to the stimulation protocols used in the experimental studies.

We found that the initial high-frequency doublets elicited by motor units are aligned with the Ca^{2+} binding kinetics of TnC to induce a powerful force response, a mechanism that could be fully accounted for by modeling Ca^{2+} movements based on the high temporal resolution imaging of cytoplasmic free Ca^{2+}.

MATERIALS AND METHODS

All experiments were approved by the Animal Ethics Committee of the University of Queensland (Ca^{2+} measurements) and the Animal Ethics Committee of the University of Western Australia (force measurements).

Fiber preparation

The isolation, culturing, and dye loading of interosseous fibers have been described in detail previously (Cully et al., 2012). 6-wk-old male C57BL/6J mice were killed by cervical dislocation, and the interosseous muscles were removed and placed in 3 ml of Dulbecco's modified Eagle's medium (glucose: 5 mM) containing 1.5 mg/ml collagenase type-1 (Sigma-Aldrich) digestion solution for 30 min at 30°C. Intact interosseous muscles were incubated overnight at 30°C in Dulbecco's modified Eagle's medium containing 5 mM glucose, 5% fetal calf serum, and 1 mg/ml penicillin and 1 mg/ml streptomycin. The muscles were then gently triturated to release single fibers.

Ca^{2+} measurements

Isolated fibers responding to field stimulation were transferred to a custom-made experimental chamber and positioned above the coverslip base. Fibers were loaded with the Mag-Fluo-4AM or Fluo-4AM (5 µM for 15 min) at room temperature in a HEPES-based Ringer solution (mM: 145 NaCl, 2.5 $CaCl_2$, 2 $MgCl_2$, 10 HEPES, 3 KCl, and 5 glucose). After the loading period, the dye containing Ringer solution was replaced with a dye-free Ringer solution containing the myosin II ATPase inhibitor *N*-benzyl-p-toluene sulphonamide (100 µM), to prevent cross-bridge cycling and associated movement artifacts. The chamber was placed above the inverted lens (63×, oil immersion) of a 5 LIVE (ZEISS). Isolated fibers were stimulated via platinum electrodes using supramaximal square wave pulses (0.3-ms duration) delivered by an SD9 square pulse stimulator (Grass Technologies Inc.). The stimulator was triggered at various time intervals using Chart 8 stimulator software in conjunction with a PowerLab data acquisition/stimulation system (ADInstruments) and a PC. The polarity of the stimulation electrodes was kept constant during experimentation. During stimulation, Ca^{2+}-related fluorescence changes were measured in line scan mode, and data were sampled every 0.111 ms (Edwards et al., 2012), unless otherwise stated. The Ca^{2+}-sensitive dyes trapped in the cytoplasm of the fibers were excited by the 488-nm line of an argon laser, and fluorescence emission was collected in the range >500 nm. Line scan image–derived fluorescence data were exported as a text file and analyzed using Excel (Microsoft).

In control measurements, fibers were activated at 70 Hz (10 stimulation pulses). Stimulation during the doublet measurements was similar to controls with the exception that the first two action potentials of the train were at 200 Hz. Doublet and control tetani were collected in the same recording. The doublet tetanus was delivered first, followed by the control tetanus, 1.2 s later. Control measurements were also made, where two consecutive control tetani were delivered 1.2 s apart. All experiments were performed at room temperature (22–24°C).

In some experiments, the effect of doublet stimulation on Ca^{2+} release was measured under conditions

similar to those reported previously by Cheng et al. (2013) using the same temporal resolution (500 Hz) and Fluo-4, which has similar affinity to Ca^{2+} as indo-1 (see Results).

To ensure only fast fibers were used in this study, only fibers exhibiting the Ca^{2+} transient shape characteristic for type IIb/IIx fibers were selected for analysis (Calderón et al., 2009, 2014).

Force measurements

Experiments assessing the impact of doublet stimulation on tetanic force responses were undertaken using isolated extensor digitorum longus (EDL) muscles from 6-wk-old male C57BL/6J mice. EDL muscles from C57BL/6J mice primarily contain fast IIb/x fibers (IIb/x fibers 88%, type IIa fibers 12%; Rinaldi et al., 2012), as used in the Ca^{2+} experiments in this study. Therefore, the use of intact muscle preparations in this study should provide a relatively accurate estimate of the effects of doublet stimulation on force production in fast IIb/x fibers.

EDL muscles (n = 8) were removed surgically under anesthesia (40 mg/kg pentobarbitone) and mounted onto an in vitro muscle test system (model 1205A; Aurora Scientific Inc.; Pinniger et al., 2012). Muscles were maintained in an organ bath containing mammalian Ringer solution (mM: 121 NaCl, 25 $NaHCO_3$, 11.5 glucose, 5.4 KCl, 2.5 $CaCl_2$, 5 HEPES, and 1 $MgSO_4$, pH 7.3) bubbled with carbogen (5% CO_2 in O_2; BOC). The Ringer was maintained at 25°C, which is reported to be optimal for the maintenance of in vitro muscle force (Segal and Faulkner, 1985). After muscles were removed, the mice were euthanized by an overdose of pentobarbitone.

Muscles were stimulated with platinum electrodes using supramaximal square wave pulses (0.3-ms duration) provided by a high-power bi-phase current stimulator (Aurora Scientific Inc.). The stimulator was triggered at various time intervals using Chart 7 stimulator software and a PowerLab data acquisition/stimulation system (ADInstruments). Before experiments commenced, muscles were set to a length producing maximum isometric twitch force (optimal muscle length). In control measurements, muscles were stimulated with 10 pulses at 70 Hz. Doublet measurements were similar except the first two action potentials were delivered at 200 Hz. 70 Hz is close to the mean motor neuron discharge rate in rodents (Hennig and Lømo, 1985; Gorassini et al., 2000). 2-min intervals were maintained between tetanic stimulations to prevent onset of muscle fatigue (Sitparan et al., 2014). Force output was recorded using a PowerLab data acquisition system and LabChart 7 software (ADInstruments).

Statistics

The data are presented as means ± SEM. Statistical analysis was undertaken using the graphical software package Prism (Graph Pad Software). The absolute amplitudes of initial Ca^{2+} spikes transients measured in the Ca^{2+} transients were compared using a paired t test. The relative change in the minimum fluorescence between Ca^{2+} spikes that occurred during the Ca^{2+} transients in control and doublet traces was compared using a repeated measures two-way ANOVA followed by a Šídák's multiple comparisons test.

Mathematical modeling

To provide insight into the mechanisms underpinning force enhancement by doublet stimulation, a mathematical model was used to describe the kinetics of Ca^{2+} distribution within muscle fibers and the generation of force. The model was based on those described earlier (Robertson et al., 1981; Baylor et al., 1983) and is summarized in Fig. 1 A. It is described by six differential equations of the form described in detail previously (Baylor and Hollingworth, 1998) and which were solved using a program developed using Maple software (version 2016.1; Maplesoft).

The concentrations of Ca^{2+} binding and other relevant compounds (Table 1) and parameter values (Table 2) used for the model were taken from Baylor and Hollingworth's (Baylor and Hollingworth, 2003, 2007, 2012) models applicable to mouse muscle fibers. The rate constants were adjusted from 16°C, as used by Baylor and Hollingworth, to 22°C assuming a Q_{10} (i.e., the increase in rate for a 10°C increase in temperature) of 2. The interaction between Ca^{2+} and the fluorescent indicator was not included in the model. Instead, it was assumed that the measured Ca^{2+} signal provided a faithful representation of the time course of the free Ca^{2+} transient; this is true for Mag-Fluo-4 (Baylor and Hollingworth, 2011). On this basis, the free Ca^{2+} transient predicted by the model was compared directly with the measured signal (Fig. 1 B).

Removal of Ca^{2+} from the myoplasm into the SR was modeled as described previously (Ríos and Brum, 2002). The rate of removal was assumed to have a sigmoidal dependence on $[Ca^{2+}]_C$, a maximum rate of 4,670 µM/s (determined empirically to achieve a good match between measured and simulated Ca^{2+} transients) and to pump at 50% of the maximum rate when $[Ca^{2+}]_C$ was 2.5 µM (Baylor et al., 2002). A small, constant rate Ca^{2+} leak from the SR of 2 nM/s was included in the model. This leak rate and the pump characteristics established a realistic resting $[Ca^{2+}]_C$ of 0.05 µM (Bakker et al., 1993). The resting $[Ca^{2+}]_C$ determines the fractions of the Ca^{2+} buffers occupied by Ca^{2+} in the muscle before stimulation.

A novel aspect of the model was incorporation of force generation. It was assumed that the formation of force-generating actomyosin cross-bridges (labeled "AM" in Fig. 1 A) was enabled by binding of the Ca^{2+} to the second binding site on TnC (Tn-Ca_2, Fig. 1; Ashley

Table 1. **Myoplasmic concentrations of Ca^{2+}, Mg, and Ca^{2+} binding compounds and concentrations expressed relative to cell water volume**

Compound	Concentration	Reference
Total Ca^{2+}	4,000 µM	Lamboley et al., 2015
Resting [Ca^{2+}]	0.05 µM (SR Ca^{2+} leak, 0.005 µM/s)	Bakker et al., 1993
Resting [Mg^{2+}]	1 mM	Barclay, 2015
ATP	8,000 µM	Barclay, 2015
Tn	120 µM; two distinct Ca^{2+}-binding sites/molecule	Baylor and Hollingworth, 2003
Pv	750 µM; two equivalent Ca^{2+}-binding sites/molecule	Raymackers et al., 2000
M	120 µM; assumed equal to [Tn]	
A	Available actin binding sites, concentration time-dependent and equal to [Tn-Ca_2]	

Where necessary, reported values expressed relative to muscle wet weight were converted by multiplying by 1.5 (Baylor et al., 1983).

Table 2. **Rate constants used in model for Ca^{2+}-binding reactions at 22°C**

Reaction	k_+	k_-
	$\mu M^{-1}\ s^{-1}$	s^{-1}
Ca^{2+} + Tn ⇆ TnCa	570	2,340
Ca^{2+} + TnCa ⇆ $TnCa_2$	133	136
Ca^{2+} + Pv ⇆ PvCa	63	1.2
Mg^{2+} + Pv ⇆ PvMg	0.05	4.6
Ca^{2+} + ATP ⇆ ATPCa	20.6	45,470
A + M ⇆ AM	0.083	22.7

k_+, forward rate constant; k_-, reverse rate constant. Rate constants for 22°C, adjusted from values used for 16°C by Baylor and colleagues (Baylor et al., 2002; Baylor and Hollingworth, 2003, 2007) assuming Q_{10} of 2.

and Moisescu, 1972). Note that the second site could only be filled once the first binding site was occupied by Ca^{2+}. The rate constants for formation and dissociation of force generating cross-bridges were set so that the predicted time course of twitch force at 16°C matched that described for mouse EDL muscle by Baylor and Hollingworth (2003). The rates were adjusted to 22°C using a Q_{10} of 2. Examples of simulated force responses are shown in Fig. 1 C.

Simulations started with all the Ca^{2+} in the SR and the leak being the only source of Ca^{2+} entry into the myoplasm. Once the occupancy of the Ca^{2+}-binding sites on ATP, TnC, and parvalbumin settled to steady values, the response to stimulation was simulated by invoking a transient release, or releases if multiple stimuli were being modeled, of Ca^{2+} from the SR with an asymmetric time course described by two exponentials, one rising and the other falling (Baylor and Hollingworth, 2012). The design of the model was validated by ensuring that it accurately reproduced Baylor and Hollingworth's simulations when using their parameter values for 16°C. Thereafter, parameters appropriate for 22°C were used.

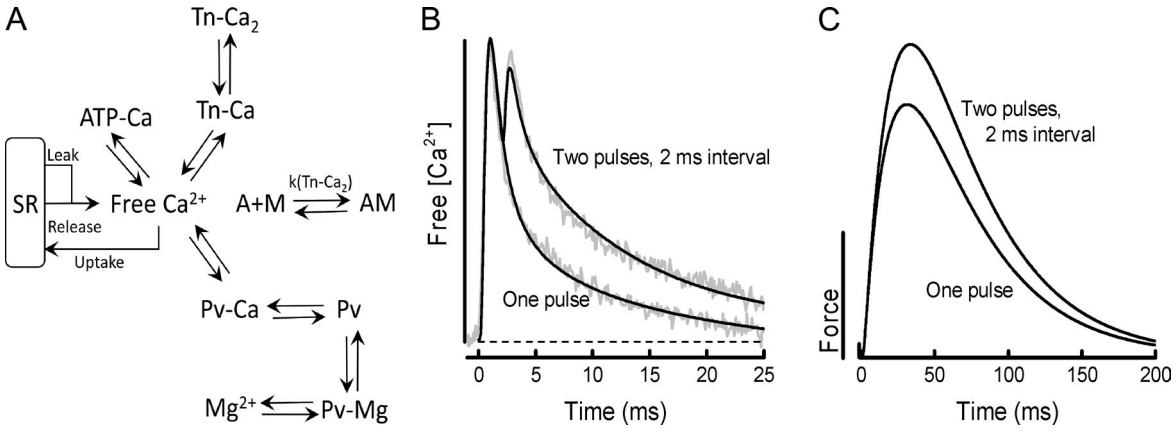

Figure 1. **Simulation of the effects of doublet stimulation on cytosolic free Ca^{2+} and force production.** (A) Graphical depiction of the model of Ca^{2+} distribution and force generation. The model incorporates both a constant Ca^{2+} leak and stimulus-induced, transient Ca^{2+} release from the SR. In the myoplasm, Ca^{2+} is distributed among (i) TnC (Tn), with two, sequentially filled Ca^{2+} binding sites, forming Tn-Ca when one Ca^{2+} is bound and Tn-Ca_2 when both sites are occupied; (ii) parvalbumin (Pv), which has two equivalent Ca^{2+}-binding sites per molecule that also bind Mg^{2+}; (iii) ATP; and (iv) unbound or free Ca^{2+}. Ca^{2+} is removed from the myoplasm via the SR Ca^{2+} pump. Force generation involves the binding of myosin cross-bridges (M) to binding sites on actin (A) to form the force-generating actomyosin complex (AM). AM formation was regulated by Tn-Ca_2, which was achieved by setting the concentration of available actin sites equal to [Tn-Ca_2]. (B) Comparison of recorded Ca^{2+} transients (gray uneven lines) and modeled free Ca transients (black smooth lines). Two records are shown, the response to a single stimulus pulse and the response to two stimulus pulses separated by 2 ms. The experimental records are the mean of records from four fibers with amplitude scaled by the maximum amplitude in response to the first stimulus pulse. (C) Simulated force responses to one pulse and to two pulses separated by 2 ms.

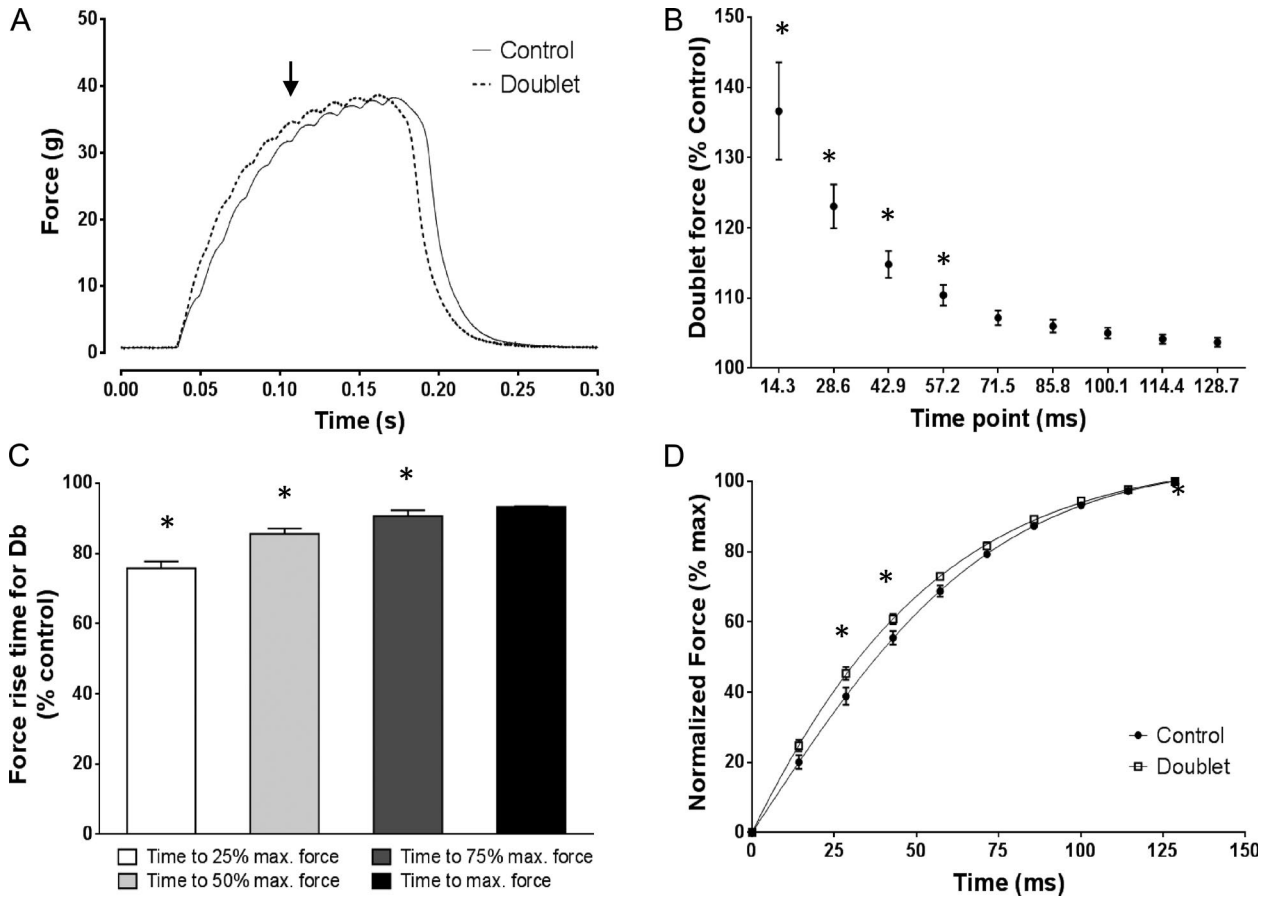

Figure 2. **Effect of the doublet stimulation (200 Hz) on tetanic force responses elicited in intact EDL muscles.** (A) An example of force traces elicited after exposure to 10 stimulation pulses at 70 Hz in the absence and presence of an initial 200-Hz doublet. The arrow shows the time point where Cheng et al. (2013) stopped stimulating their intact fiber preparation and shows why a difference in peak force was observed in that study and not the present study; i.e., force had not plateaued in Cheng et al. (2013). (B) The effect of doublet stimulation on peak force production (% control) at different time points during the tetanic force response. (C) The effect of doublet stimulation on normalized force production (% of maximal force). (D) The time taken for the doublet force response to rise to 25%, 50%, 75%, and 100% of maximum force, expressed as a percentage of the control response. Data are presented as means ± SEM. *, $P < 0.05$.

RESULTS

We initially measured the effect of a 200-Hz doublet pulse on force output in isolated intact EDL muscle exposed to tetanic stimulation (10 pulses, 70 Hz). Doublet stimulation indeed resulted in force responses that increased more rapidly and to higher levels than controls (Fig. 2 A). Doublet stimulation significantly decreased the rise time of the force response (Fig. 2 B) and significantly increased the level of force output from the muscle for at least the first 57 ms (Fig. 2 C). The presence of a doublet also shifted the relationship between normalized force and time to the left (Fig. 2 D; $P < 0.05$), indicating that the rate constant of force development is significantly increased in the doublet responses. Note that the final level of force in the doublet and control responses was similar. We note that previous studies have used shorter overall periods of stimulation (the arrow on Fig. 2 A indicates the end of stimulation in Cheng et al. (2013), which emphasize the effects of doublet stimulation on peak force during the early phase of the force response (Cheng et al., 2013).

We then examined the effects of 200-Hz doublet stimulation on tetanic (70 Hz) Ca^{2+} release under similar conditions to Cheng et al. (2013) (i.e., using a high-affinity Ca^{2+} indicator and sampling at 500 Hz). However, we used laser-scanning microscopy instead of photometry and the Ca^{2+} indicator Fluo-4 instead of indo-1. Fluo-4 (K_d for Ca^{2+}: ~345 nM; Paredes et al., 2008) has a similar reported affinity for Ca^{2+} to indo-1 (K_d for Ca^{2+}: ~250 nM; Grynkiewicz et al., 1985). At 500-Hz sampling frequency, we found a qualitatively similar apparent increase in the initial peak Ca^{2+}-related fluorescence after doublet stimulation to that reported previously by Cheng et al. (2013) (Fig. 3, representative of three experiments). However, with the enhanced signal-to-noise of laser-scanning microscopy compared with photometry (Edwards et al., 2012), it was possible to resolve indi-

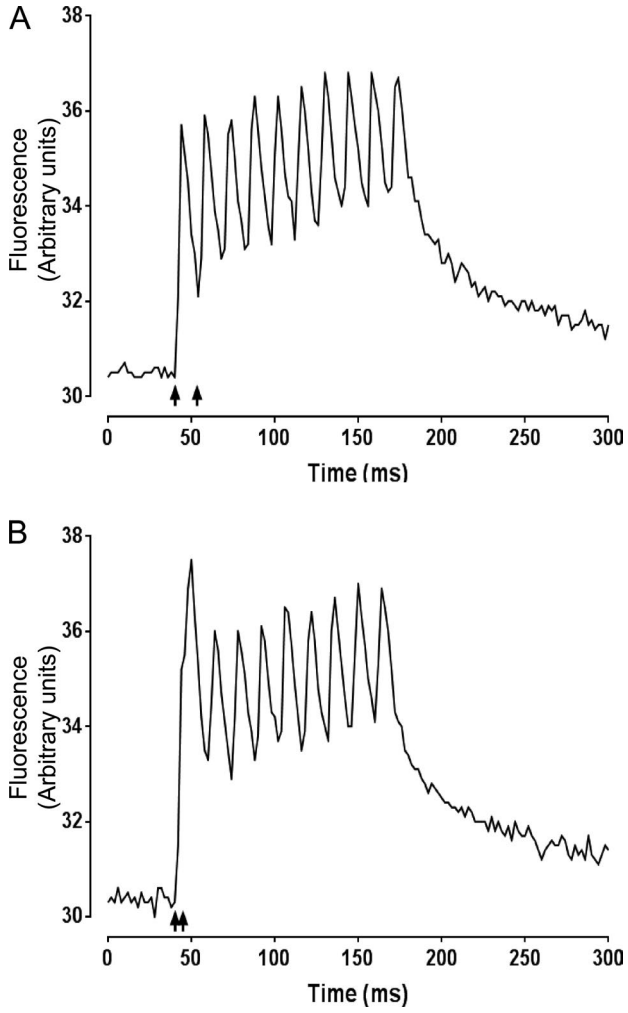

Figure 3. **Effect of doublet stimulation on Ca^{2+} transients measured in interosseous fibers using Fluo-4 at a sampling frequency of 500 Hz.** Arrows indicate timing of the first two stimulation pulses. (A and B) Fibers were exposed to 10 stimulation pulses at 70 Hz in the absence (A) and presence (B) of an initial 200-Hz doublet stimulation.

vidual Ca^{2+} spikes within the tetanus. In the control tetanus, each of the 10 stimulation events resulted in individual Ca^{2+} spikes (Fig. 3 A), whereas in the doublet transient, the 10 stimulation pulses resulted in only nine peaks (Fig. 3 B). The apparent fusion of the initial two Ca^{2+} transient peaks activated by the doublet (Fig. 3 B) is a likely result of sampling below the Nyquist frequency.

To verify that our imaging system (5 LIVE; ZEISS) was capable of accurately tracking $[Ca^{2+}]_C$ (t) during high-frequency stimulation in fast-twitch muscle fibers, we line-scanned isolated fibers at 111 µs/line using the low-affinity Ca^{2+} indicator Mag-Fluo-4, while applying twin field pulses in the range 200–1,000 Hz. The use of a low-affinity dye at high temporal resolution allowed the $[Ca^{2+}]_C$ (t) to be resolved, as clearly shown by the twin Ca^{2+} spikes at each stimulation frequency (Fig. 4 A). Furthermore, importantly, in each case the secondary stimulus did not produce a Ca^{2+} peak higher than that triggered by the first. This indicates that the amount of Ca^{2+} released by the first action potential must be significantly greater than the second, suggesting that CDI was occurring under these conditions.

The amount of Ca^{2+} released in response to the second of a pair of stimuli was quantified using the model of Ca^{2+} kinetics (described in Materials and methods). This was undertaken by iteratively scaling the amount of Ca^{2+} released in response to the second pulse until a match was achieved between the amplitudes of the measured and simulated Ca^{2+} transient peaks arising from the second stimulus. A comparison of the experimental and simulated Ca^{2+} transients is provided in Fig. 5 (A and B) and the relative Ca^{2+} release in response to the second of the two stimuli is shown in Fig. 5 C. The analysis indicates that the amount of Ca^{2+} released by the second stimulus pulse, expressed relative to that released by the first stimulus, was between 15 and 25%, for pulse intervals between 1 and 4 ms. A small addition of Ca^{2+} to the myoplasm by the second stimulus produced a relatively large Ca^{2+} transient because the fiber's rapid Ca^{2+}-buffering capacity is reduced by the binding of Ca^{2+} released by the first stimulus to TnC, ATP, and parvalbumin. The simulated force responses (Fig. 5 D) showed that a second stimulus could increase peak force by ∼30% compared with the response to a single stimulus. The basis of this effect, in terms of the model used, is a doublet-induced increase in the fraction of TnC molecules with two Ca^{2+} bound to the regulatory binding sites (Fig. 5, E and, in more detail, F). After a single stimulus, the proportion of TnC with 2 Ca^{2+} bound reached a peak of 60%; this was increased to 70% by the addition of a second stimulus pulse 2 ms after the first (Fig. 5 F).

We then imaged Ca^{2+} transients during control and doublet tetani using the stimulation protocol of Cheng et al. (2013) under the conditions established in Fig. 4 A. Control tetani at 70 Hz resulted in Ca^{2+} transients that were similar in shape to those reported previously for fast type IIb/IIx fibers under similar conditions (Fig. 6 A; Calderón et al., 2011). When a 200-Hz doublet stimulus was inserted at the start of the tetanus, a second Ca^{2+} spike was clearly delineable from the first spike (Fig. 6 B). In all fibers, the initial single large Ca^{2+} spike was followed by Ca^{2+} spikes that did not reach a peak higher than the initial one (Fig. 6, A and B). The main effect of doublet stimulation was to minimize the drop in $[Ca^{2+}]_{cyto}$ (t) between the first three Ca^{2+} spikes in the doublet response (Fig. 6 C). There was no significant difference in the amplitude of the initial Ca^{2+} spike elicited after doublet or control stimulation (initial doublet Ca^{2+} spike: 111.6 ± 4.2% of initial control 70-Hz response; $n = 6$).

The basis of the effects of the doublet stimulation on Ca^{2+} transients and force development were analyzed

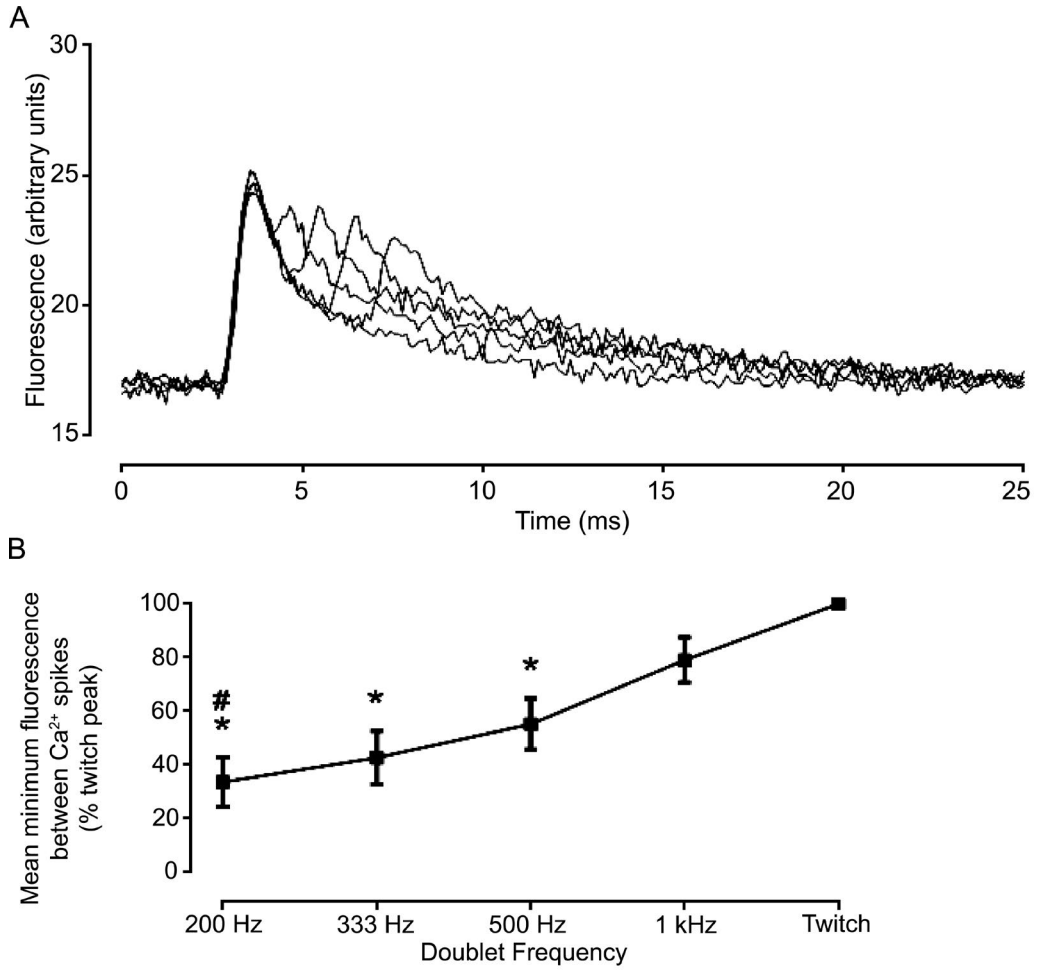

Figure 4. **Effect of stimulation frequency on doublet-induced changes in cytoplasmic free Ca^{2+}.** (A) An overlay of a Ca^{2+} transient activated by a single stimulation pulse and various doublet Ca^{2+} transients measured at stimulation frequencies ranging from 200 Hz to 1 kHz. Measurements were made using the low-affinity Ca^{2+} indicator Mag-Fluo-4 and confocal line scanning at 111 μs/line. (B) The minimum fluorescence between Ca^{2+} spikes expressed as a percentage of the peak of the Ca^{2+} transient activated by a single stimulation pulse (*, significantly different to 1 kHz; #, significantly different to 500 Hz; $n = 4$ fiber; $P < 0.05$). Data are presented as means ± SEM.

using the model. As discussed in the Introduction, the interval between stimulus pulses affects the amount of Ca^{2+} released in response to the second, and subsequent, pulses. With constant 70-Hz stimulation, 45% as much Ca^{2+} was released by the second stimulus as by the first. In contrast, using the doublet stimulation pattern with the first and second pulses 5 ms apart, the second pulse liberated only 33% as much Ca^{2+} as the first pulse. The effects of this on the binding of Ca^{2+} to TnC, which underlies force development, are shown in Fig. 7 B. After the initial high-frequency doublet, the concentration of TnC molecules with both Ca^{2+}-binding sites occupied is greater between 5 and 15 ms after the first stimulus than with constant frequency stimulation (Fig. 7 B, compare dashed and solid lines). This translated into more rapid force development; the modeling indicated that the time taken for force to develop to 50% of maximum is reduced with doublet stimulation from 31 to 23 ms (Fig. 7 D). The simulation further shows that the more rapid increase in force is sustained so that force output was higher throughout the 150 ms of stimulation (Fig. 7 D, inset). As expected, Ca^{2+} release measurements showed a greater CDI-related decrease in SR Ca^{2+} release in response to the second stimulus pulse of the doublet tetani compared with the control; however, Ca^{2+} release in the doublet response returned to control levels shortly after and remained similar to controls for the rest of the response (Fig. 7 E).

DISCUSSION

The results of this study show that 200-Hz doublet stimulation results in significant increases in the rate of force development and the initial amplitude of resulting force responses, leading to the powerful "ballistic" contractions reported previously under these condi-

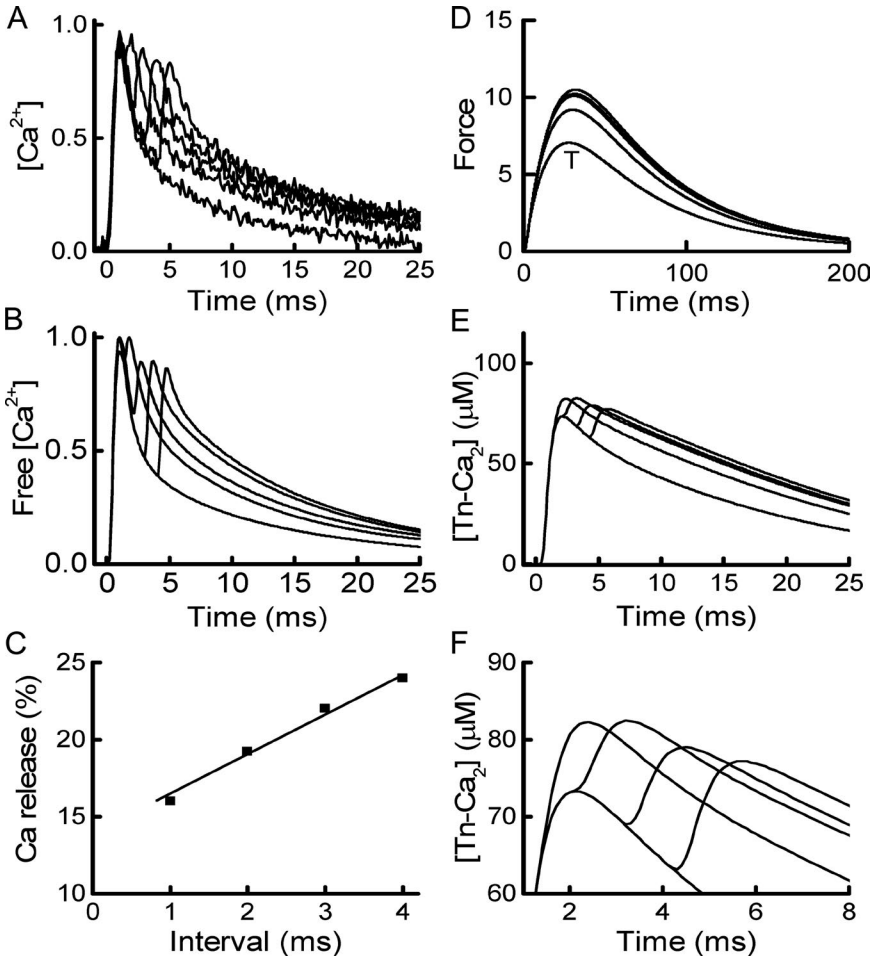

Figure 5. **Analysis of Ca^{2+} transients in response to pairs of pulses.** (A) Averaged records of $[Ca^{2+}]_C$ in response to a single pulse (lower record) and pairs of pulses at 1-, 2-, 3-, and 4-ms intervals. Each record is the mean of records from four fibers normalized by peak value in response to first stimulus. (B) Simulated time courses of free $[Ca^{2+}]$ in response to the same stimulus patterns used for A. (C) Amount of Ca^{2+} released in response to second stimulus expressed relative to that released by first pulse. (D) Simulated time courses of force output in response to a single stimulus (labeled "T") or pairs of pulses (upper traces). Note the different time scale to other graphs. (E) Simulated time courses of the concentration of TnC with two Ca^{2+} bound ($Tn\text{-}Ca_2$). The total concentration of sites is 120 μM. (F) Detail from E, highlighting the increase in $[Tn\text{-}Ca_2]$. Provision of a second stimulus increased above that achieved in a twitch and close to saturation (i.e., $[Tn\text{-}Ca_2]$ = 120 μM).

tions (Desmedt and Godaux, 1977; Van Cutsem et al., 1998). However, our findings indicate that high-frequency doublet stimulation does not result in an increase in peak free Ca^{2+} in fast-twitch skeletal muscle fibers, in contrast to previous studies (Duchateau and Hainaut, 1986; Abbate et al., 2002; Cheng et al., 2013), but maintains a higher $[Ca^{2+}]_C$ (t) for the first 20 ms of the tetanic Ca^{2+} transient (Figs. 4, 5, 6, and 7).

Simulation of the changes in Ca^{2+} binding to the main intracellular Ca^{2+} buffers during tetanic Ca^{2+} release shows that the main effect of the second response in the doublet is to more rapidly increase occupation of the second Ca^{2+}-binding site on TnC (TnC_2), beyond that which was achieved by the first Ca^{2+} release response. The increase in the rate of force development shown in this study (Fig. 2 D) ultimately reflects the higher occupancy of TnC_2 rather than a change in the rate constant for cross-bridge attachment per se, in terms of the model used in this study. The increased rate of force development reflects the increased modulation of the rate constant for cross-bridge attachment and force generation induced by the earlier increase in the concentration of TnC_2. Although the second pulse of the doublet increases saturation of TnC_2 with Ca^{2+}, considerably less Ca^{2+} is actually released in response to the second pulse in the doublet compared with that released by the second pulse in a pair of constant, lower-frequency pulses (Fig. 5 C). However, because of the extent of saturation of the rapid Ca^{2+} buffers (TnC and ATP) by the first pulse in the doublet, even a relatively small addition of Ca^{2+} to the myoplasm in response to the second pulse is sufficient to prevent a significant decrease in $[Ca^{2+}]_C$ and to increase the fraction of TnC molecules with two Ca^{2+} bound. Earlier occupation of Ca^{2+}-binding sites on the other cytosolic Ca^{2+} buffers, after doublet stimulation (Fig. 7 C), would also slow the rate of post-release Ca^{2+} decay (Baylor and Hollingworth, 2003) and consequently prolong Ca^{2+} occupancy of TnC, further contributing to the faster rate of force development after doublet stimulation.

Increased saturation of TnC_2 underpins the more rapid development of force in response to doublet stimulation, as shown in the modeled force responses in Fig. 5 D, which are in close agreement with the effects of doublet stimulation on force enhancement in intact fast-twitch muscles in vitro (Fig. 2 A). It should be noted that although our results indicate that doublet stimulation has no effect on peak tetanic plateau force production (10 stimulation pulses; Fig. 2 A), stimulation bursts with a smaller number of pulses, such as those typically

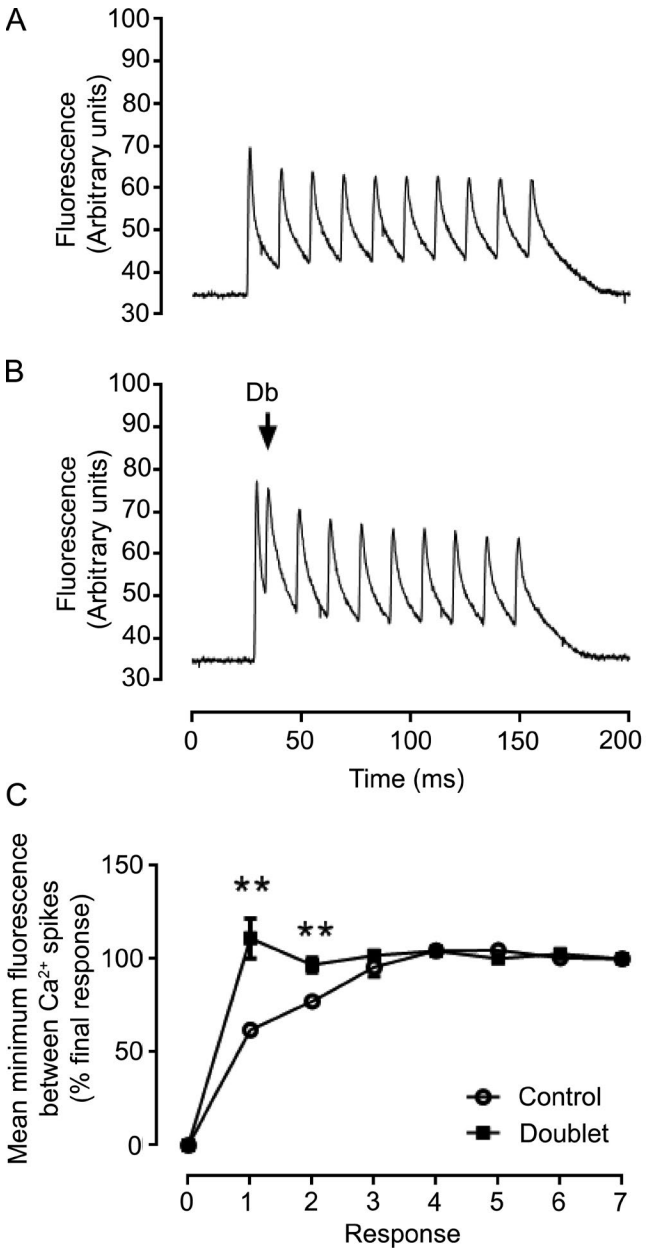

Figure 6. **The effect of doublet stimulation (200 Hz) on Ca^{2+} transients measured in interosseous fibers using Mag-Fluo-4 (sampling every 111 µs) during tetanic activation at 70 Hz.** (A) Stimulation at 70 Hz resulted in Ca^{2+} transients that exhibited a larger initial Ca^{2+} spike, after which peak Ca^{2+} gradually decreased to a uniform lower level. The minimum fluorescence values between Ca^{2+} spikes (expressed as a percentage of the minimum fluorescence between the final two Ca^{2+} spikes in the Ca^{2+} transient) gradually increased to a plateau. (B) The presence of a doublet (Db), indicated by the arrow, produced two clear Ca^{2+} spikes in response to the doublet action potentials, but had no effect on peak Ca^{2+}. (B and C) Doublet stimulation resulted in a persistent increase in the minimum fluorescence values between the initial three Ca^{2+} spikes (**, significantly different to control, $P < 0.01$). Data are presented as means ± SEM.

found in fast-fatigable motor units (Hennig and Lømo, 1985), will increase peak tetanic force output, as shown in Cheng et al. (2013).

Modeling of the effects of high-frequency doublets on Ca^{2+} release shows that CDI is extremely rapid in fast twitch fibers, markedly decreasing Ca^{2+} release during the second response of the doublet to 15–20% of initial SR Ca^{2+} in <1 ms (Fig. 5 C). The degree of CDI found in this study under tetanic conditions, where Ca^{2+} release during the second pulse of burst was ∼33% of the first for the doublet (5-ms pulse interval) or 45% of the first for controls (15-ms pulse interval), was very similar to the values reported recently by using a different experimental approach (Barclay, 2012). Barclay (2012) estimated SR Ca^{2+} release during tetanic stimulation from ATP turnover–derived SR Ca^{2+} reuptake measurements made in the absence of cross-bridge cycling and found that Ca^{2+} release during the second pulse of a tetanus was ∼30% of that occurring in response to the first pulse for a 5-ms pulse interval and ∼40% of the first for a 15-ms pulse interval. The values found here are also in the same range as those reported by Baylor and Hollingworth (2007), who developed the modeling methodology used in this study, where 25% as much Ca^{2+} was released in response to the second stimulus compared with the first for a 15-ms interpulse period (based on Ca^{2+} transients measured at 16°C). The results of this study also indicate that the magnitude of CDI elicited by the doublet (5-ms pulse interval) returns to control levels by the third pulse of the 10-pulse protocol and remains relatively constant during the rest of the response, in keeping with previous findings using different methodology (Barclay, 2012). Overall, these results suggest that CDI provides a finely tuned negative feedback mechanism that matches SR Ca^{2+} release to inter-pulse stimulus duration, in order to provide the minimum Ca^{2+} release required to maintain significant occupation of TnC_2 with Ca^{2+}.

In this study, we showed that fibers responded to stimulation frequencies of up to 1 KHz with two clear Ca^{2+} release events (Fig. 4 A), which to the best of our knowledge is the first time this ability has been reported in skeletal muscle. However, our simulation data suggest that doublet stimulation rates in the range 200–1,000 Hz will all result in similar increases in TnC_2 binding (see Figs. 5 E and 7 B), suggesting that doublet frequencies >300 Hz would not further increase force enhancement (Fig. 5 D) and would be of little functional value. In keeping with this, doublet frequencies in vivo are usually around 200 Hz. For example, in humans, mean doublet frequencies have been shown to be around 180 Hz (Christie and Kamen, 2006), whereas in fast muscle of rats, mean doublet frequencies between 160 and 290 Hz have been reported (Gorassini et al., 2000). In fact, high doublet frequencies (>250 Hz) may be detrimental. Burke et al. (1976) measured muscle force output and electromyography (EMG) in response to motor-neuron doublet stimulation and reported a decrease in force enhancement and a reduction in the EMG response to the second stimulation pulse at pulse intervals

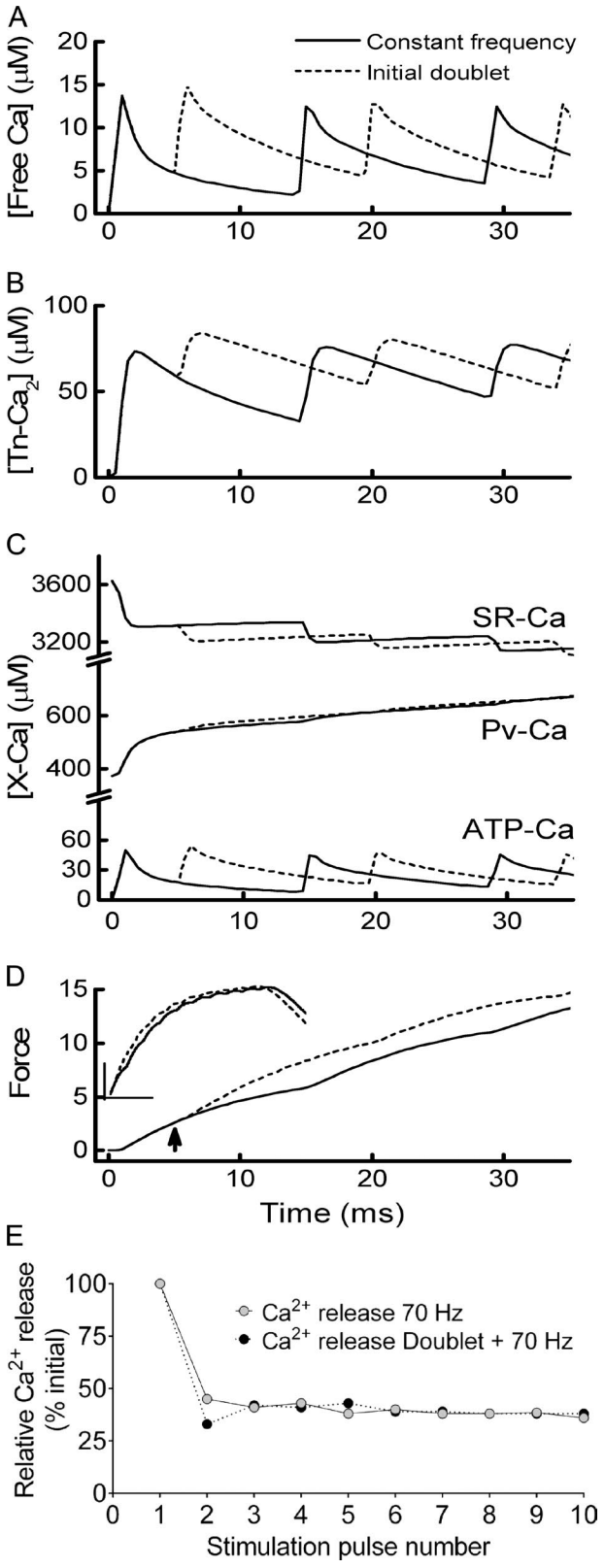

Figure 7. **Simulated responses to constant frequency and doublet stimulation.** Simulations of constant frequency stimulation (70 Hz) are shown with solid lines, and simulations of the response to doublet stimulation (two pulses at 200 Hz followed by eight at 70 Hz) are shown with broken lines. (A) Free Ca^{2+}. The time scale encompasses the first three stimuli only. (B) Concentration of TnC with both Ca^{2+}-binding regulatory sites occupied by Ca^{2+}. (C) Concentration of Ca^{2+} in the SR and bound to parvalbumin (Pv) and bound to ATP. (D) Force output during the initial force development. The more rapid force development in response to the doublet stimulation is apparent. The arrow indicates the time at which the second stimulus was delivered in the doublet protocol. The inset shows the time course of force development for 150 ms after the first stimulus, encompassing all 10 stimuli delivered. (E) SR Ca^{2+} release as a percentage of initial Ca^{2+} release in response to constant frequency and doublet stimulation during the 10-pulse tetanic stimulus.

of 4 ms or less. Given that our findings indicate the loss of EMG is unlikely to be caused by an inability of the fiber to react to the second stimulus, higher frequency doublets may be ineffective because of a failure of neurotransmission at these high stimulation frequencies, at least in sedentary animals.

In summary, the results of this study show that doublet stimulation results in maintained higher values of $[Ca^{2+}]_C$ (t) during the early portion of tetanic Ca^{2+} release (Fig. 6 C). Our results and others (Baylor and Hollingworth, 2007, 2012) indicate that the enhancement of skeletal muscle force production can be fully explained by the increased Ca^{2+} availability in the cytoplasm resulting from doublet stimulation and its main effect to rapidly increase the saturation of TnC_2. Finally, these findings do not support the existence of any doublet-induced "catch-like" process of force enhancement in fast-twitch skeletal muscle. Rather, doublet activation works through the normal force-summation mechanism, where it acts to significantly increase the rate of force development during the early phase of contraction and, presumably, more powerful force responses under isotonic conditions. Therefore, a more appropriate description than catch-like for the effects of doublet stimulation on force production would be doublet-induced rapid summation.

ACKNOWLEDGMENTS

This work was supported by the Sabbatical Leave Program of the University of Western Australia to A.J. Bakker and an Australian Research Council (ARC) Discovery Project to B.S. Launikonis. B.S. Launikonis was a Future Fellow of the ARC.

The authors declare no competing financial interests.

Author contributions: A.J. Bakker: conceptualization, investigation, methodology, formal analysis, writing–original draft, and writing–review and editing. T.R. Cully: investigation, methodology, and writing–review and editing. C.D. Wingate: investigation, formal analysis, and writing–review and editing. C.J. Barclay: conceptualization, investigation, methodology, formal analysis, and writing–review and editing. B.S. Launikonis: conceptualization, investigation, methodology, formal analysis, and writing–review and editing.

Eduardo Ríos served as editor.

Submitted: 17 November 2016
Accepted: 9 January 2017

REFERENCES

Abbate, F., J.D. Bruton, A. De Haan, and H. Westerblad. 2002. Prolonged force increase following a high-frequency burst is not due to a sustained elevation of $[Ca^{2+}]_i$. *Am. J. Physiol. Cell Physiol.* 283:C42–C47. http://dx.doi.org/10.1152/ajpcell.00416.2001

Ashley, C.C., and D.G. Moisescu. 1972. Model for the action of calcium in muscle. *Nat. New Biol.* 237:208–211. http://dx.doi.org/10.1038/newbio237208a0

Bakker, A.J., S.I. Head, D.A. Williams, and D.G. Stephenson. 1993. Ca2+ levels in myotubes grown from the skeletal muscle of dystrophic (mdx) and normal mice. *J. Physiol.* 460:1–13. http://dx.doi.org/10.1113/jphysiol.1993.sp019455

Barclay, C.J. 2012. Quantifying Ca^{2+} release and inactivation of Ca^{2+} release in fast- and slow-twitch muscles. *J. Physiol.* 590:6199–6212. http://dx.doi.org/10.1113/jphysiol.2012.242073

Barclay, C.J. 2015. Energetics of contraction. *Compr. Physiol.* 5:961–995. http://dx.doi.org/10.1002/cphy.c140038

Baylor, S.M., and S. Hollingworth. 1998. Model of sarcomeric Ca^{2+} movements, including ATP Ca^{2+} binding and diffusion, during activation of frog skeletal muscle. *J. Gen. Physiol.* 112:297–316. http://dx.doi.org/10.1085/jgp.112.3.297

Baylor, S.M., and S. Hollingworth. 2003. Sarcoplasmic reticulum calcium release compared in slow-twitch and fast-twitch fibres of mouse muscle. *J. Physiol.* 551:125–138. http://dx.doi.org/10.1113/jphysiol.2003.041608

Baylor, S.M., and S. Hollingworth. 2007. Simulation of Ca^{2+} movements within the sarcomere of fast-twitch mouse fibers stimulated by action potentials. *J. Gen. Physiol.* 130:283–302. http://dx.doi.org/10.1085/jgp.200709827

Baylor, S.M., and S. Hollingworth. 2011. Calcium indicators and calcium signalling in skeletal muscle fibres during excitation-contraction coupling. *Prog. Biophys. Mol. Biol.* 105:162–179. http://dx.doi.org/10.1016/j.pbiomolbio.2010.06.001

Baylor, S.M., and S. Hollingworth. 2012. Intracellular calcium movements during excitation-contraction coupling in mammalian slow-twitch and fast-twitch muscle fibers. *J. Gen. Physiol.* 139:261–272. http://dx.doi.org/10.1085/jgp.201210773

Baylor, S.M., W.K. Chandler, and M.W. Marshall. 1983. Sarcoplasmic reticulum calcium release in frog skeletal muscle fibres estimated from Arsenazo III calcium transients. *J. Physiol.* 344:625–666. http://dx.doi.org/10.1113/jphysiol.1983.sp014959

Baylor, S.M., S. Hollingworth, and W.K. Chandler. 2002. Comparison of simulated and measured calcium sparks in intact skeletal muscle fibers of the frog. *J. Gen. Physiol.* 120:349–368. http://dx.doi.org/10.1085/jgp.20028620

Binder-Macleod, S., and T. Kesar. 2005. Catchlike property of skeletal muscle: recent findings and clinical implications. *Muscle Nerve.* 31:681–693. http://dx.doi.org/10.1002/mus.20290

Burke, R.E., P. Rudomin, and F.E. Zajac III. 1970. Catch property in single mammalian motor units. *Science.* 168:122–124. http://dx.doi.org/10.1126/science.168.3927.122

Burke, R.E., P. Rudomin, and F.E. Zajac III. 1976. The effect of activation history on tension production by individual muscle units. *Brain Res.* 109:515–529. http://dx.doi.org/10.1016/0006-8993(76)90031-7

Calderón, J.C., P. Bolaños, S.H. Torres, G. Rodríguez-Arroyo, and C. Caputo. 2009. Different fibre populations distinguished by their calcium transient characteristics in enzymatically dissociated murine flexor digitorum brevis and soleus muscles. *J. Muscle Res. Cell Motil.* 30:125–137. http://dx.doi.org/10.1007/s10974-009-9181-1

Calderón, J.C., P. Bolaños, and C. Caputo. 2011. Kinetic changes in tetanic Ca^{2+} transients in enzymatically dissociated muscle fibres under repetitive stimulation. *J. Physiol.* 589:5269–5283. http://dx.doi.org/10.1113/jphysiol.2011.213314

Calderón, J.C., P. Bolaños, and C. Caputo. 2014. Tetanic Ca^{2+} transient differences between slow- and fast-twitch mouse skeletal muscle fibres: a comprehensive experimental approach. *J. Muscle Res. Cell Motil.* 35:279–293. http://dx.doi.org/10.1007/s10974-014-9388-7

Capote, J., P. Bolaños, R.P. Schuhmeier, W. Melzer, and C. Caputo. 2005. Calcium transients in developing mouse skeletal muscle fibres. *J. Physiol.* 564:451–464. http://dx.doi.org/10.1113/jphysiol.2004.081034

Cheng, A.J., N. Place, J.D. Bruton, H.C. Holmberg, and H. Westerblad. 2013. Doublet discharge stimulation increases sarcoplasmic reticulum Ca^{2+} release and improves performance during fatiguing contractions in mouse muscle fibres. *J. Physiol.* 591:3739–3748. http://dx.doi.org/10.1113/jphysiol.2013.257188

Christie, A., and G. Kamen. 2006. Doublet discharges in motoneurons of young and older adults. *J. Neurophysiol.* 95:2787–2795. http://dx.doi.org/10.1152/jn.00685.2005

Cully, T.R., J.N. Edwards, O. Friedrich, D.G. Stephenson, R.M. Murphy, and B.S. Launikonis. 2012. Changes in plasma membrane Ca-ATPase and stromal interacting molecule 1 expression levels for Ca^{2+} signaling in dystrophic mdx mouse muscle. *Am. J. Physiol. Cell Physiol.* 303:C567–C576. http://dx.doi.org/10.1152/ajpcell.00144.2012

Desmedt, J.E., and E. Godaux. 1977. Ballistic contractions in man: characteristic recruitment pattern of single motor units of the tibialis anterior muscle. *J. Physiol.* 264:673–693. http://dx.doi.org/10.1113/jphysiol.1977.sp011689

Duchateau, J., and K. Hainaut. 1986. Nonlinear summation of contractions in striated muscle. II. Potentiation of intracellular Ca^{2+} movements in single barnacle muscle fibres. *J. Muscle Res. Cell Motil.* 7:18–24. http://dx.doi.org/10.1007/BF01756198

Edwards, J.N., T.R. Cully, T.R. Shannon, D.G. Stephenson, and B.S. Launikonis. 2012. Longitudinal and transversal propagation of excitation along the tubular system of rat fast-twitch muscle fibres studied by high speed confocal microscopy. *J. Physiol.* 590:475–492. http://dx.doi.org/10.1113/jphysiol.2011.221796

Gorassini, M., T. Eken, D.J. Bennett, O. Kiehn, and H. Hultborn. 2000. Activity of hindlimb motor units during locomotion in the conscious rat. *J. Neurophysiol.* 83:2002–2011.

Grynkiewicz, G., M. Poenie, and R.Y. Tsien. 1985. A new generation of Ca^{2+} indicators with greatly improved fluorescence properties. *J. Biol. Chem.* 260:3440–3450.

Hennig, R., and T. Lømo. 1985. Firing patterns of motor units in normal rats. *Nature.* 314:164–166. http://dx.doi.org/10.1038/314164a0

Lamboley, C.R., S.A. Kake Guena, F. Touré, C. Hébert, L. Yaddaden, S. Nadeau, P. Bouchard, L. Wei-LaPierre, J. Lainé, E.C. Rousseau, et al. 2015. New method for determining total calcium content in tissue applied to skeletal muscle with and without calsequestrin. *J. Gen. Physiol.* 145:127–153. http://dx.doi.org/10.1085/jgp.201411250

Paredes, R.M., J.C. Etzler, L.T. Watts, W. Zheng, and J.D. Lechleiter. 2008. Chemical calcium indicators. *Methods.* 46:143–151. http://dx.doi.org/10.1016/j.ymeth.2008.09.025

Pinniger, G.J., T. Lavin, and A.J. Bakker. 2012. Skeletal muscle weakness caused by carrageenan-induced inflammation. *Muscle Nerve.* 46:413–420. http://dx.doi.org/10.1002/mus.23318

Raymackers, J.M., P. Gailly, M.C. Schoor, D. Pette, B. Schwaller, W. Hunziker, M.R. Celio, and J.M. Gillis. 2000. Tetanus relaxation of fast skeletal muscles of the mouse made parvalbumin deficient by gene inactivation. *J. Physiol.* 527:355–364. http://dx.doi.org/10.1111/j.1469-7793.2000.00355.x

Rinaldi, M., K. Maes, S. De Vleeschauwer, D. Thomas, E.K. Verbeken, M. Decramer, W. Janssens, and G.N. Gayan-Ramirez. 2012. Long-term nose-only cigarette smoke exposure induces emphysema

and mild skeletal muscle dysfunction in mice. *Dis. Model. Mech.* 5:333–341. http://dx.doi.org/10.1242/dmm.008508

Ríos, E., and G. Brum. 2002. Ca^{2+} release flux underlying Ca^{2+} transients and Ca^{2+} sparks in skeletal muscle. *Front. Biosci.* 7:d1195–d1211.

Robertson, S.P., J.D. Johnson, and J.D. Potter. 1981. The time-course of Ca2+ exchange with calmodulin, troponin, parvalbumin, and myosin in response to transient increases in Ca2+. *Biophys. J.* 34:559–569. http://dx.doi.org/10.1016/S0006-3495(81)84868-0

Segal, S.S., and J.A. Faulkner. 1985. Temperature-dependent physiological stability of rat skeletal muscle in vitro. *Am. J. Physiol.* 248:C265–C270.

Sitparan, P.K., C.N. Pagel, G.J. Pinniger, H.J. Yoo, E.J. Mackie, and A.J. Bakker. 2014. Contractile properties of slow and fast skeletal muscles from protease activated receptor-1 null mice. *Muscle Nerve.* 50:991–998. http://dx.doi.org/10.1002/mus.24256

Van Cutsem, M., J. Duchateau, and K. Hainaut. 1998. Changes in single motor unit behaviour contribute to the increase in contraction speed after dynamic training in humans. *J. Physiol.* 513:295–305. http://dx.doi.org/10.1111/j.1469-7793.1998.295by.x

Zehr, E.P., and D.G. Sale. 1994. Ballistic movement: muscle activation and neuromuscular adaptation. *Can. J. Appl. Physiol.* 19:363–378. http://dx.doi.org/10.1139/h94-030